

## Density Functional Study on Phenol Derivative–Ammonia Complexes in the Gas Phase

Agnieszka J. Abkowitz-Bieńko and Zdzisław Latajka\*

Faculty of Chemistry, University of Wrocław, ul. Joliot-Curie 14, 50-383 Wrocław, Poland

Received: September 8, 1999; In Final Form: November 10, 1999

Ab initio calculations with the DFT/BLYP level of theory and the 6-31G(d,p) basis set were performed on the hydrogen-bonded phenol derivative–ammonia complexes. Phenol and its following four derivatives with growing acidity, *p*-nitrophenol, pentafluorophenol, 2,6-difluoro-4-nitrophenol, and 2-fluoro-4,6-dinitrophenol, were considered. The parameters sensitive to hydrogen bonding as well as their changes due to complex formation were studied. The calculated frequencies of phenol–ammonia complex showed good overall agreement with the recently reported experimental data. Thus, it is concluded that infrared spectra predicted for the other complexes studied in this work, at the same theory level, are also correct. The OH stretch vibrations of the phenol derivative moieties have showed large red shifts from that of isolated phenol, whereas the OH torsion vibrations have shifted toward higher wavenumbers. Despite the growing acidity of investigated phenols, no proton transfer toward ammonia was observed.

### Introduction

Hydrogen-bonded complexes involving phenol have been the subject of numerous studies by means of both molecular beam spectroscopy experiments<sup>1–20,27</sup> and theoretical investigations.<sup>1,3,21–25</sup>

The interest in phenol derivatives hydrogen bonding has several motivations. As phenol is the simplest aryl alcohol, its hydrogen-bonding interactions can serve as a prototype for the interaction of larger, biological species (e.g., tyrosine residues in proteins). Moreover, changing the substituent results in a large increase in acidity. This growth allows, under some circumstances, the occurrence of proton transfer to proton-accepting solvent species such as water or ammonia. Such proton transfer has been observed for phenol complexes with proton acceptors upon electronic excitation into its first singlet electronic state.<sup>17,18</sup>

Compared to its water analogue, there are relatively few papers on the phenol–amine systems.<sup>1,17,26,27,29–37</sup> Moreover, neither theoretical nor experimental systematic work on phenol derivative–ammonia complexes has been published up to now. The properties of the phenol derivative–amine complexes depend on the position of the proton in the hydrogen bridge. Phenol derivatives with high values of  $pK_a$  (weak acids) are characterized to form the molecular hydrogen bonded complexes (O–H···B), whereas growing acidity (low  $pK_a$  values) allow to form ion pair (O<sup>−</sup>···H<sup>+</sup>–B) structures. The tautomeric equilibrium is possible for medium acidity. The situation described above is well-known and was studied both for liquid state<sup>32–34</sup> and low-temperature matrices.<sup>35</sup> The question arises as to what the situation will be in the gas phase. Does the proton transfer occur due to the growth of acidity?

In the present work, we perform the density functional study at the BLYP/6-31G(d,p) level on phenol and its four derivatives (*p*-nitrophenol, pentafluorophenol, 2,6-difluoro-4-nitrophenol, and 2-fluoro-4,6-dinitrophenol) forming hydrogen-bonded complexes with ammonia subunit. The change of the functional groups and their position in the phenyl ring gives the possibility to get a wide range of  $pK_a$  values, which may cause, as was

shown for the solution and the condensed phase, the proton transfer toward the proton acceptor moiety. Using the DFT/BLYP method lets us provide relatively reliable information on the nature of interactions as well as vibrational spectra of investigated complexes. Thus, we performed calculations to obtain information about the structures, energetics, and nature of interactions between phenols and ammonia in the gas phase. We focus mainly on the parameters as well as vibrational frequencies sensitive to hydrogen bridge formation.

It is demonstrated that frequencies calculated at the BLYP/6-31G(d,p) level, for the phenol–NH<sub>3</sub> system, are in very good agreement with the experimental data obtained by jet-cooled spectroscopy.<sup>26,27</sup> Moreover, in our previous paper<sup>28</sup> we have reported detailed study of the infrared spectrum of phenol using Hartree–Fock, MP2 and DFT/BLYP method and 6-31G(d,p) basis set. It has been demonstrated that of the three methods the BLYP functional best reproduced the vibrational spectrum of the phenol. The MP2/6-31G(d,p) method failed in predicting two vibrations of the aromatic ring, labeled 14 and 4, whereas calculation at the HF/6-31G(d,p) level provided incorrect results for the modes related to the OH in-plane bending vibration in phenol. Thus, it is anticipated that the predicted infrared spectra for the complexes formed between other investigated phenols and ammonia, at the same theory level, should be reliable. In order to get an insight into the nature of vibrational modes, we performed the normal-coordinate analysis, which enabled us to obtain a detailed interpretation of the vibrational spectra of the investigated molecules.

### Computational Details

The density functional method with the BLYP functional calculations were performed using the 6-31G(d,p) basis set with the Gaussian 94/DFT program.<sup>38</sup>

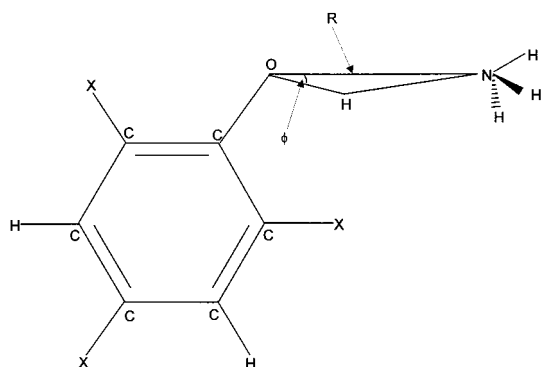
The geometry optimizations of all the monomers considered as well as complexes with ammonia were performed under relaxation of all internal degrees of freedom, assuming planarity of the complexes (*C<sub>s</sub>* symmetry). The harmonic vibrational frequencies were subsequently calculated using the numerical differentiation of analytical gradients. The approximate assign-

\* Corresponding author. E-mail: latajka@wchuwr.chem.uni.wroc.pl.

**TABLE 1: Comparison of Calculated Parameters Sensitive to the Hydrogen Bond Formation for the Phenol Derivatives–Ammonia Complexes with Growing Acidity<sup>a</sup> (Bond Lengths in Å, Angles in deg, Energies in kcal/mol)**

|                                    | phenol          |                 |                  |                  |                   | <i>p</i> -nitrophenol<br>BLYP <sup>f</sup> | pentafluorophenol<br>BLYP <sup>f</sup> | 2,6-difluoro-4-nitrophenol<br>BLYP <sup>f</sup> | 2-fluoro-4,6-dinitrophenol<br>BLYP <sup>f</sup> |
|------------------------------------|-----------------|-----------------|------------------|------------------|-------------------|--|--|---|---|
|                                    | HF <sup>b</sup> | HF <sup>c</sup> | MP2 <sup>d</sup> | MP2 <sup>e</sup> | BLYP <sup>f</sup> |  |  |   |   |
| $r(\text{OH})$                     | 0.954           | 0.996           | 0.994            | 0.987            | 1.004             | 1.014                                      | 1.023                                  | 1.030   | 1.040   |
| $\Delta r(\text{OH})$              |                 | 0.016           | 0.020            | 0.020            | 0.027             | 0.034                                      | 0.055                                  | 0.049   | 0.056   |
| $R(\text{O}\cdots\text{N})$        | 2.952           |                 | 2.840            |                  | 2.824             | 2.775                                      | 2.721                                  | 2.700   | 2.666   |
| $r(\text{C}-\text{O})$             | 1.341           | 1.364           | 1.365            | 1.364            | 1.365             | 1.352                                      | 1.350                                  | 1.341   | 1.328   |
| $\Delta r(\text{C}-\text{O})$      |                 | -0.013          | -0.012           | -0.014           | -0.017            | -0.018                                     | -0.021                                 | -0.021  | -0.024  |
| $\theta(\text{COH})$               | 112.30          | 116.4           |                  |                  | 110.77            | 111.67                                     | 113.56                                 | 113.60  | 115.08  |
| $\varphi(\text{OH}\cdots\text{N})$ | 6.3             | 8.3             | 8.9              | 8.9              | 6.3               | 6.15                                       | 5.57                                   | 5.15  | 8.49  |
| $\Delta E^{\text{CP}}$             | -8.53           |                 | -6.03            | -6.03            | -7.45             | -10.13                                     | -11.03                                 | -11.86  | -13.12  |
| $\Delta E_{\text{dep}}^{\text{g}}$ |                 |                 |                  |                  | 364.4             | 345.5                                      | 337.7                                  | 331.23  | 319.64  |
| $\text{p}K_{\text{a}}$             |                 |                 |                  |                  | 10.0              | 7.16                                       | 5.53 (4.47) <sup>h</sup>               | (3.55) <sup>h</sup>                             | (2.1) <sup>h</sup>                              |

<sup>a</sup> Full list of geometrical parameters as well as frequencies are available from the authors on the request. <sup>b</sup> From ref 26, calculated with the 6-31G(d,p) basis set; the value interaction energy is not corrected for BSSE. <sup>c</sup> From ref 27, calculated with the 6-31G basis set. <sup>d</sup> From ref 32, calculated with the D95(d) basis set. <sup>e</sup> From ref 33, calculated with the DZP basis set. <sup>f</sup> This work. <sup>g</sup>  $\Delta E_{\text{dep}}$  is the deprotonation energy calculated as a difference of energy for phenol derivative and its deprotonated analogue. <sup>h</sup> Values in parentheses are related to chloroderivatives of phenol due to the lack of experimental data.

**Figure 1.** Structure of phenol derivative–ammonia complexes optimized at DFT/6-31G(d,p) level with BLYP functional.

ments were done according to normal-coordinate analysis using the ab initio calculated Cartesian force constants as an input.<sup>39</sup>

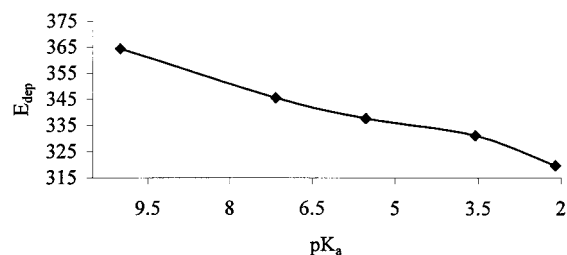
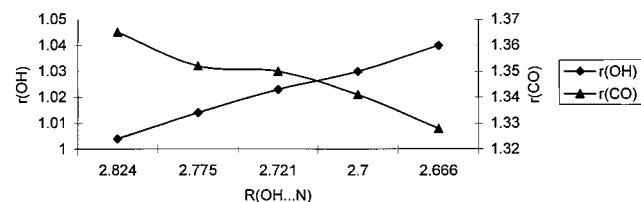
Interaction energies, calculated as the difference of total energy between the complex and the monomers, were basis set superposition error (BSSE) corrected using the standard Boys–Bernardi procedure.<sup>40</sup>

## Structure

The optimized structures of the investigated complexes are of the  $C_s$  symmetry with one ammonia hydrogen atom lying in the aromatic plane and two other placed symmetrically above and below the plane (Figure 1). Because of sterical effects, the out-of-plane hydrogens reside on the cis side of the hydrogen-bond axis.

As the bond lengths and angles related to phenolic ring are not particularly sensitive to the formation of the hydrogen bond, we focus mainly on the structural parameters involved into intermolecular interactions. The results are presented in Table 1 along with earlier calculated data for phenol– $\text{NH}_3$  complex.<sup>26,27,33</sup>

Shiefke et al.<sup>26</sup> as well as Iwasaki et al.<sup>27</sup> have carried out ab initio calculations and provided an energy-optimized structure for the phenol–ammonia complex. They have used, however, the HF level of theory, which neglects the electron correlation necessary for the proper description of the hydrogen-bonding systems. Moreover, Iwasaki et al. used the basis set without polarization functions. Thus, some differences in optimized parameters are observed (Table 1). As follows from Table 1, the results calculated at the DFT/BLYP level with the 6-31G(d,p) basis set showed a good overall agreement with those obtained at MP2/D95(d) level.<sup>32</sup> Since the proton donor

**Figure 2.** Correlation between  $\text{p}K_{\text{a}}$  values and deprotonation energies for studied phenol derivatives.**Figure 3.** Correlation between the OH bond length and CO bond length of the phenol derivative–ammonia complexes and the intermolecular distances.

character increases along with the growth of acidity, the systematic elongation of the OH bond length, due to the complex formation ( $\Delta r(\text{OH})$ ), is observed. At the same time, as expected, the systematic shortening of the CO bond is noted. The changes described above correlated reasonably with acidity which reflect in  $\text{p}K_{\text{a}}$  values. Although the value of  $\text{p}K_{\text{a}}$  is related to acidity in the liquid phase, it correlates excellently with the calculated deprotonation energies, which can be seen in Figure 2. The correlations for both the elongation of the OH bond length and the shortening of the CO bond length versus the  $(\text{OH}\cdots\text{N})$  distance are presented in Figure 3. Despite the continuous elongation of the OH bond length, due to the growth of acidity, no proton transfer is observed in the studied systems.

The length of the hydrogen bond defined by the distance between heavy atoms (O and N) is substantially larger for the phenol–ammonia complex than for the other investigated systems. The distance of 2.824 Å is typical for  $\text{O}-\text{H}\cdots\text{N}$  hydrogen bonding.<sup>41</sup> Consistent with that value is the  $\text{O}\cdots\text{N}$  distance of 2.77 Å for 2-naphthol–ammonia complex obtained by rotationally resolved laser-induced fluorescence (LIF) measurements,<sup>42</sup> as well as the experimental value determined for the  $\text{H}_2\text{O}-\text{NH}_3$  complex (2.98 Å).<sup>43</sup> Moreover, a similar value has been theoretically predicted at the MP2/D95(d) level.<sup>32</sup> The increasing strength of the hydrogen bond is reflected in the values of interaction energy going from the complex formed

**TABLE 2: Calculated Intermolecular Frequencies (in  $\text{cm}^{-1}$ ) for the Phenol Derivative–Ammonia Complexes<sup>a</sup>**

|           | phenol           |                 |                 |                  |                    | <i>p</i> -nitrophenol<br>B3LYP <sup>g</sup> | pentafluorophenol<br>B3LYP <sup>g</sup> | 2,6-difluoro-<br>4-nitrophenol<br>B3LYP <sup>g</sup> | 2-fluoro-4,6-<br>dinitrophenol<br>B3LYP <sup>g</sup> |                    |
|-----------|------------------|-----------------|-----------------|------------------|--------------------|---|---|--|--|--------------------|
|           | exp <sup>b</sup> | HF <sup>c</sup> | HF <sup>d</sup> | MP2 <sup>e</sup> | B3LYP <sup>f</sup> |   |   |  |  | B3LYP <sup>g</sup> |
| $\rho_1$  |                  | 31              | 35              | 38               | 33                 | 35  | 22                                      | 20   | 22   | 31                 |
| $\tau$    |                  | 37              | 39              | 41               | 62                 | 55  | 33                                      | 44   | 51   | 36                 |
| $\beta_1$ | 60               | 64              | 67              | 66               | 68                 | 69  | 63                                      | 95   | 94   | 90                 |
| $\sigma$  | 164              | 165             | 184             | 188              | 202                | 197   | 190                                     | 187  | 202  | 202                |
| $\rho_2$  |                  | 242             | 291             | 284              | 287                | 270   | 308                                     | 294  | 318  | 328                |
| $\beta_2$ | 322              | 305             | 355             | 322              | 329                | 314   | 333                                     | 442  | 447  | 467                |

<sup>a</sup> Abbreviations:  $\rho_1$ ,  $\rho_2$ , rocking,  $\tau$ , torsion;  $\beta_1$ ,  $\beta_2$ , wagging,  $\sigma$ , hydrogen bond stretching. Full list of geometrical parameters as well as frequencies are available from the authors on the request. <sup>b</sup> Experimental values obtained by jet-cooled spectroscopy in supersonic jets from ref 29. <sup>c</sup> From ref 26, calculated with the 6-31G(d,p) basis set. <sup>d</sup> From ref 27, calculated with the 6-31G basis set. <sup>e</sup> From ref 32, calculated with the D95(d) basis set. <sup>f</sup> From ref 33, calculated with the DZP basis set. <sup>g</sup> This work.

**TABLE 3: Experimental and Calculated Values of the OH Stretching and Torsion Vibrations for the Phenol Derivative–Ammonia Complexes**

|                       | phenol            |                   |          |                | <i>p</i> -nitrophenol |                | pentafluorophenol |                | 2,6-difluoro-4-nitrophenol |                | 2-fluoro-4,6-dinitrophenol |                |
|-----------------------|-------------------|-------------------|----------|----------------|-----------------------|----------------|-------------------|----------------|----------------------------|----------------|----------------------------|----------------|
|                       | exp               |                   | calc     |                | calc                  |                | calc              |                | calc                       |                | calc                       |                |
|                       | $\nu$             | $\Delta\nu$       | $\omega$ | $\Delta\omega$ | $\omega$              | $\Delta\omega$ | $\omega$          | $\Delta\omega$ | $\omega$                   | $\Delta\omega$ | $\omega$                   | $\Delta\omega$ |
| OH <sub>stretch</sub> | 3294 <sup>a</sup> | −469 <sup>b</sup> | 3156     | −508           | 3006                  | −648           | 2851              | −780           | 2730                       | −886           | 2593                       | −980           |
| OH <sub>tors</sub>    | 822 <sup>c</sup>  |                   | 882      | 498            | 961                   | 559            | 976               | 578            | 1034                       | 564            | 1087                       | 544            |

<sup>a</sup> From ref 28. <sup>b</sup> From ref 27. <sup>c</sup> From ref 1.

between the weakest acid and ammonia to the strongest one. As follows from Table 1, the interaction energy corrected for BSSE changes from  $-7.45$  to  $-13.12$  kcal/mol.

The intermolecular distance for the other complexes studied in this work are shorter due to the higher acidity of the phenol derivative involved in the hydrogen bonding. For example, the distance in the 2-fluoro-4,6-dinitrophenol–ammonia ( $R = 2.666$  Å) complex is definitely smaller than in the phenol–ammonia system ( $R = 2.824$  Å). This result is consistent with the hydrogen bond in 2-fluoro-4,6-dinitrophenol–ammonia being much stronger than that in phenol–NH<sub>3</sub>.

The hydrogen bonds in phenol derivative–ammonia complexes are distorted from a linear arrangement by  $5^\circ$ – $8^\circ$  (see Table 1). The distortion is the largest for the strongest hydrogen bond (2-fluoro-4,6-dinitrophenol). The deviation from linearity for the phenol–NH<sub>3</sub> complex, calculated at the DFT/BLYP level, is somewhat smaller compared to the MP2/D95(d) level. It may be either an effect of DFT or the result of the smaller basis set used. On the other hand, its value is slightly larger than for the phenol–H<sub>2</sub>O complex ( $3.3^\circ$  at the HF/6-31G(d,p) level)<sup>44</sup> due to the stronger sterical interaction in complexes with ammonia than with water molecule.

### Vibrational Spectra

Since the detailed interpretation of the vibrational spectra was not the main focus of our investigations we have concentrated only on the vibrations sensitive to the hydrogen-bond formation. Moreover, the assignment for low-frequency intermolecular vibration has been made. The investigated bands for the phenol–NH<sub>3</sub> complex have been compared to existing experimental data<sup>29</sup> as well as the results recently calculated by Re et al.<sup>33</sup> and others.<sup>26,27,32</sup>

Because of the hydrogen-bond interaction between phenol derivatives and ammonia, six intermolecular vibrations arise. The calculated harmonic DFT(BLYP)/6-31G(d,p) frequencies are presented in Table 2. Two of them are the rocking modes of  $A''$  symmetry, and the next two are wagging modes of  $A'$  symmetry. Moreover, one  $A''$  torsion mode and the  $A'$  hydrogen bond stretch are present. According to the nomenclature published by Schütz et al.,<sup>44</sup> the rocking modes, approximately

perpendicular to the phenol molecular plane, are denoted  $\rho_1$  and  $\rho_2$ , the wagging modes, parallel to the phenol plane,  $\beta_1$  and  $\beta_2$ , the torsion mode  $\tau$  around the hydrogen bond axis, and the hydrogen bond stretching mode  $\sigma$ .

Since the vibrations labeled  $\rho_2$ ,  $\tau$ , and  $\beta_2$  have small reduced masses as well as small frequencies and therefore large vibrational amplitudes, they are expected to be inappropriately described within the harmonic approximation.<sup>25,44</sup> Nevertheless, the lack of experimental values for  $\rho_1$  and  $\tau$  bands, due to their low intensities, hinders corroboration of that fact.

It was noted previously for the phenol–H<sub>2</sub>O complex that the anharmonic correction for the  $\beta_2$  mode is important.<sup>44</sup> However, both our calculations and the work published earlier<sup>32</sup> showed that for the phenol–NH<sub>3</sub> complex, the  $\beta_2$  harmonic value is in nearly perfect agreement with experimental data. Similar results were obtained recently at B3LYP/DZP level.<sup>33</sup> Although it can be the result of error cancellation, it seems that in this case the anharmonic correction is not necessary.

On the other hand, for the vibrations denoted  $\sigma$ ,  $\beta_1$ , and  $\rho_1$ , the harmonic approximation gives relatively good agreement with experimental values as was presented previously for the phenol–H<sub>2</sub>O complex.<sup>21,44</sup> Moreover, the harmonic description turned out to be quite reasonable in reproducing both  $\beta_1$  and H-bond stretch  $\sigma$  in the phenol–NH<sub>3</sub> complex as can be seen from Table 2.

The calculated intermolecular O···N stretch frequencies ( $\sigma$ ) are close to the value of  $200 \text{ cm}^{-1}$  and are in the range normally expected for the hydrogen-bonded complexes in the gas phase. Moreover, detailed analysis of the values presented in Table 2 shows very small blue shifts when going to the more acidic phenol derivative, and the relation with the interaction energy is not linear. It is difficult to explain this fact but anharmonic effects may play some role.

In summary, the intermolecular frequencies calculated at the BLYP/6-31G(d,p) level for the phenol–ammonia system are in quite good overall agreement with available experimental data, which confirms the reliability of the present band assignment for the concerned bands in other investigated complexes. Thus, it is concluded that the predicted infrared spectrum for the phenol–NH<sub>3</sub> complexes, shown in Table 2, should also be reliable.

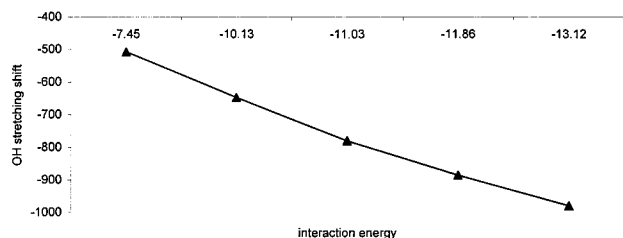


**Figure 4.** Correlation between red shift of the OH stretching vibrations and interaction energies of studied complexes.

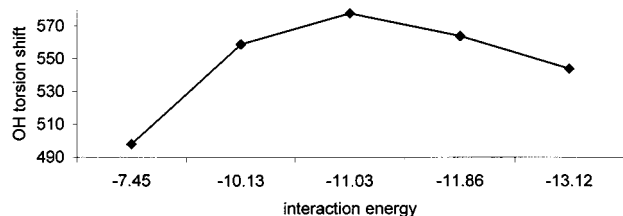


**Figure 5.** Correlation between the blue shift of the OH torsion vibrations and interaction energies of studied complexes.

With respect to the intramolecular modes, the most sensitive due to the hydrogen bonding are OH stretching, bending, and torsion modes. The OH bending vibration, however, is strongly coupled with other vibrations. As the  $\beta$ -OH normal mode contributes to several bands and its percent contribution to them is not significant, the assignment is not unique. Thus, we concentrate on the frequencies connected with OH stretch and torsion vibrations. As can be seen from Table 3, the frequency shifts, associated with the  $A''$  torsional mode and the  $A'$  stretching mode, are large. The computed shift of the OH stretching mode in the phenol– $\text{NH}_3$  system with respect to that in isolated phenol<sup>28</sup> ( $-508 \text{ cm}^{-1}$ ) is larger than the value obtained experimentally for this complex<sup>27</sup> ( $-469 \text{ cm}^{-1}$ ). On the basis of this comparison, one can conclude that the predicted frequencies for OH stretching mode in the other complexes are also slightly overestimated. It can be seen, however, that the calculated values are reasonably correlated with the strength of the hydrogen bond in investigated complexes.

Since the acidities of phenols increase, this result suggests a correlation of red shifts of hydrogen-bonded OH stretching frequencies with respect to the interaction energies of investigated complexes. Such correlation is presented in Figure 4 and seems to be close to linear. Similar correlation between the shift of the hydrogen-bonding OH stretching frequencies and proton affinities of proton acceptor subunits were presented for phenol–amine clusters in the condensed phase.<sup>1,27</sup> It supports that the OH frequency shift is an indicator of the hydrogen bond strength.

The excellent correlation between the  $\Delta\omega(\text{OH}_{\text{stretch}})$  and  $E^{\text{CP}}$  also indicates that it is not necessary to take into account proton transfer along the hydrogen bond bridge. The occurrence of PT would perturb the correlation by replacing the hydrogen-bonding OH stretching vibrations by NH stretching vibration having a different frequency. Similar conclusion has been drawn from the study on phenol–amine clusters.<sup>27</sup>

Furthermore, the correlation of the OH torsion vibration shift and the proton donor properties could be expected. As follows from Table 3 the blue shift, which is in range  $490\text{--}580 \text{ cm}^{-1}$ , occur with the complex formation. In this case, however, the changes are not linear. The correlation is presented in Figure 5. The maximum value is related to the pentafluorophenol–ammonia complex. Although the 2,6-difluoro-4-nitrophenol–ammonia complex is stronger than both *p*-nitrophenol–ammonia

and pentafluorophenol–ammonia systems, it is structurally related to the latter and therefore the values of OH torsion shift for these complexes are of similar value. Because of the steric effects as well as the influence of nitro substituent, the OH torsion shift for the 2-fluoro-4,6-dinitrophenol–ammonia complex is smaller than for the rest of the complexes formed by other substituted phenols. Moreover, in the two strongest systems, namely 2,6-difluoro-4-nitrophenol–ammonia complex and 2-fluoro-4,6-dinitrophenol–ammonia complex, the distance between the OH group hydrogen and fluorine atom is about  $2 \text{ \AA}$ , which suggests the intramolecular hydrogen bond formation.

## Conclusions

1. All the phenol derivatives considered in this study form relatively strong hydrogen-bonded complexes with ammonia subunit. The growth of acidity of proton donors, as indicated by the experimental  $\text{p}K_{\text{a}}$  values as well as by the calculated deprotonation energies, reflects in the increase of binding energy. For all the complexes studied, the hydrogen bridge is almost linear.

2. The geometrical parameters related to the phenolic ring are not particularly sensitive to the hydrogen-bonding formation. Only for the OH and CO bond lengths, significant changes are observed. Despite successive elongations of the OH bond lengths along with the shortening of CO bond lengths, no proton transfer is noted for phenol–amine complexes in the gas phase. All investigated complexes are of molecular type.

3. The calculations for the phenol–ammonia complex reproduce the experimentally obtained large red shifts of the OH stretching mode of the proton donor subunit. Moreover, the calculated  $\Delta\omega_{\text{OH}}$  follows the increased strength of hydrogen-bonded complexes and almost linear correlation between the  $\Delta\omega_{\text{OH}}$  and  $\Delta E^{\text{CP}}$  of phenol–amine is observed.

**Acknowledgment.** The authors thank the Poznań Supercomputer and Networking Center as well as Wrocław Supercomputer and Networking Center for a generous computer time grant. Dariusz C. Bieńko is thanked for helping us with PED calculations.

## References and Notes

- (1) Hartland, G. V.; Henson, B. F.; Venturo, V. A.; Felker, P. M. *J. Phys. Chem.* **1992**, *96*, 1164.
- (2) Abe, H.; Mikami, N.; Ito, M. *J. Phys. Chem.* **1982**, *86*, 1768.
- (3) Abe, H.; Mikami, N.; Ito, M.; Udagawa, Y. *J. Phys. Chem.* **1982**, *86*, 2567.
- (4) Abe, H.; Mikami, N.; Ito, M.; Udagawa, Y. *Chem. Phys. Lett.* **1982**, *93*, 217.
- (5) Oikawa, A.; Abe, H.; Mikami, N.; Ito, M. *J. Phys. Chem.* **1987**, *87*, 5083.
- (6) Gonohe, N.; Abe, H.; Mikami, N.; Ito, M. *J. Phys. Chem.* **1985**, *89*, 3642.
- (7) Ito, M. *J. Mol. Struct.* **1988**, *177*, 173.
- (8) Ebata, T.; Furukawa, M.; Suzuki, T.; Ito, M. *J. Opt. Soc. Am., B* **1990**, *7*, 1890.
- (9) Fuke, K.; Kaya, K. *Chem. Phys. Lett.* **1982**, *91*, 311.
- (10) Fuke, K.; Kaya, K. *Chem. Phys. Lett.* **1983**, *94*, 97.
- (11) Fuke, K.; Yoshiuchi, H.; Kaya, K.; Achiba, Y.; Sato, K.; Kimura, K. *Chem. Phys. Lett.* **1984**, *108*, 179.
- (12) Sur, A.; Johnson, P. M. *J. Phys. Chem.* **1986**, *84*, 1206.
- (13) Kneee, J. L.; Khundkar, L. R.; Zewail, A. H. *J. Chem. Phys.* **1987**, *87*, 115.
- (14) Lipert, R. J.; Bermudez, G.; Colson, S. D. *J. Phys. Chem.* **1988**, *92*, 3801.
- (15) Lipert, L. J.; Colson, S. D. *J. Chem. Phys.* **1989**, *89*, 4579.
- (16) Lipert, R. J.; Colson, S. D. *Chem. Phys. Lett.* **1989**, *161*, 303.
- (17) Solgadi, D.; Jouviet, C.; Tramer, A. *J. Phys. Chem.* **1988**, *92*, 3313.
- (18) Steadman, J.; Syage, J. A. *J. Chem. Phys.* **1990**, *92*, 4630.
- (19) Stanley, R. J.; Castelman, A. W. *J. Chem. Phys.* **1991**, *94*, 7744.

- (20) Reiser, G.; Dopfer, O.; Lindner, R.; Henri, G.; Müller-Detlefs, K.; Schlag, E. W.; Colson, S. D. *Chem. Phys. Lett.* **1991**, *181*, 1.
- (21) Honegger, E.; Bombach, R.; Leutwyler, S. *J. Chem. Phys.* **1986**, *85*, 1234.
- (22) Pohl, M.; Schmitt, M.; Kleinermanns, K. *J. Chem. Phys.* **1991**, *94*, 1717.
- (23) Schütz, M.; Bürghi, T.; Leutwyler, S. *Theochem* **1992**, *276*, 117.
- (24) Schütz, M.; Bürghi, T.; Leutwyler, S. *J. Chem. Phys.* **1993**, *98*, 3763.
- (25) Gerhards, M.; Beckman, K.; Kleinermanns, K. *Z. Phys. D.* **1994**, *29*, 223.
- (26) Schiefke, A.; Deussen, C.; Jacoby, C.; Gerhards, M.; Schmitt, M.; Kleinermanns, K.; Hering, P. *J. Chem. Phys.* **1995**, *102*, 9197.
- (27) Iwasaki, A.; Fujii, A.; Watanabe, T.; Ebata, T.; Mikami, N. *J. Phys. Chem.* **1996**, *100*, 16053.
- (28) Michalska, D.; Bieńko, D. C.; Abkowicz-Bieńko, A. J.; Latajka, Z. *J. Phys. Chem.* **1996**, *100*, 17786.
- (29) Mikami, N.; Okabe, A.; Suzuki, I. *J. Phys. Chem.* **1988**, *92*, 1858.
- (30) Jouvét, C.; Lardeux-Dedonder, C.; Richard-Viard, M.; Solgadi, D.; Tramer, A. *J. Phys. Chem.* **1990**, *94*, 5041.
- (31) Crepin, C.; Tramer, A. *Chem. Phys.* **1991**, *156*, 281.
- (32) Sodupe, M.; Oliva, A.; Bertran, J. *J. Phys. Chem. A* **1997**, *101*, 9142.
- (33) Re, S.; Osamura, Y. *J. Phys. Chem.* **1988**, *102*, 3798.
- (34) Ratajczak, H.; Sobczyk, L. *J. Chem. Phys.* **1969**, *50*, 556.
- (35) Ilczyszyn, M.; Ratajczak, H.; Ladd, J. A. *Chem. Phys. Lett.* **1988**, *153*, 385.
- (36) Ilczyszyn, M.; Ratajczak, H.; Ladd, J. A. *J. Mol. Struct.* **1989**, *198*, 499.
- (37) Wierzejewska, M.; Ratajczak, H. *J. Mol. Struct.* **1997**, *416*, 121.
- (38) Frisch, M. J.; Trucks, G. W.; Schlegel, H. B.; Gill, P. M. W.; Johnson, B. G.; Robs, M. A.; Cheeseman, J. R.; Keith, T.; Petersson, J. A.; Montgomery, K.; Raghavachari, K.; Al-Lacham, M. A.; Zakrzewski, V. G.; Ortiz, J. V.; Foresman, J. B.; Peng, C. Y.; Ayala, P. Y.; Chen, W.; Wong, M. W.; Andres, J. L.; Replogle, E. S.; Gomperts, R.; Martin, R. L.; Fox, D. J.; Binkley, J. S.; DeFrees, D. J.; Baker, J.; Stewart, J. P.; Head-Gordon, M.; C. Gonzales, C.; Pople, J. A. *Gaussian 94*, revision B.3; Gaussian Inc.: Pittsburgh, PA, 1995.
- (39) Nowak, M.; Lapiński, L., the program for normal-mode analysis.
- (40) Boys, S. F.; Bernardi, F. *Mol. Phys.* **1970**, *19*, 553.
- (41) Pimentel, G. C.; McClellan, A. L. *The Hydrogen Bond*; W. H. Freeman: San Francisco, 1960.
- (42) Plusquellic, D. F.; Tan, X-Q.; Pratt, D. W. *J. Chem. Phys.* **1992**, *96*, 8026.
- (43) Herbine, P.; Dyke, T. R. *J. Chem. Phys.* **1985**, *83*, 3768.
- (44) Schütz, M.; Bürghi, T.; Leutwyler, S.; Fischer, T. *J. Chem. Phys.* **1993**, *98*, 3763.